NASA Technical Memorandum 81549

N80-27699
(NASA-TM-81549) STARVED ELASTOHYDRODYNAMIC LUBRICATED ELLIPTICAL CONTACTS (NASA) 23 p HC A02/MF A01 CSCL 13I
Unclas
G3/37 28070

STARVED ELASTOHYDRODYNAMIC LUBRICATED ELLIPTICAL CONTACTS

Bernard J. Hamrock
Lewis Research Center
Cleveland, Ohio

Lecture 3 of a series given at the
University of Luleå, Luleå, Sweden,
July 24-August 16, 1980

STARVED ELASTOHYDRODYNAMIC LUBRICATED ELLIPTICAL CONTACTS

Bernard J. Hamrock

National Aeronautics and Space Administration
Lewis Research Center
Cleveland, Ohio 44135

E-507

It was not until the late 1960's and early 1970's that the influence of lubricant starvation on elastohydrodynamic behavior received serious consideration. Before this time it was assumed that inlets were always fully flooded. This assumption seemed to be entirely reasonable in view of the minute quantities of lubricant required to provide an adequate film. However, in due course it was recognized that some machine elements suffered from lubricant starvation.

How partial filling of the inlet to an elastohydrodynamic conjunction influences pressure and film thickness can readily be explored theoretically by adopting different starting points for the inlet pressure boundary. Orcutt and Cheng (1966) appear to have been the first to proceed in this way for a specific case corresponding to a particular experimental situation. Their results showed that lubricant starvation lessened the film thickness. Wolveridge, et al. (1971) used a Grubin (1949) approach in an analysis of starved, elastohydrodynamically lubricated line contacts. Wedeven, et al. (1971) analyzed a starved condition in a ball-on-plane geometry. Castle and Dowson (1972) presented a range of numerical solutions for the starved line-contact elastohydrodynamic situation. In these references the analyses yielded values of the proportional reduction in film thickness from the fully flooded condition in terms of a dimensionless inlet boundary parameter.

In this lecture, 15 cases in addition to the 3 presented in lecture 2 are used for hard EHL contacts and 18 cases in addition to the 3 presented in lecture 2 are used for soft EHL contacts in a theoretical study of the influence of lubricant starvation on film thickness and pressure. From the results for both hard and soft EHL contacts a simple and important dimensionless inlet boundary distance is specified. This inlet boundary distance defines whether a fully flooded or a starved condition exists in the contact. Furthermore it was found that the film thickness for a starved condition could be written in dimensionless terms as a function of the inlet distance parameter and the film thickness for a fully flooded condition. Contour plots of pressure and film thickness in and around the contact are shown for fully flooded and starved conditions. This lecture makes extensive use of the work presented by Hamrock and Dowson (1977) and Hamrock and Dowson (1979).

FULLY FLOODED -- STARVED BOUNDARY

Figure 1 shows the computing area in and around the Hertzian contact. In this figure the coordinate X is made dimensionless with respect to the semiminor axis b of the contacting ellipse, and the coordinate Y is made dimensionless with respect to the semimajor axis a of the contact ellipse. The ellipticity parameter k is defined as the semimajor axis divided by the semiminor axis of the contact ellipse ($k = a/b$). Because of the dimensionless form of the coordinates X and Y the Hertzian contact ellipse becomes a Hertzian circle regardless of the value of k. This Hertzian contact circle is shown in figure 1 with a radius of unity. The edges of the computing area, where the pressure is assumed to be ambient, are also denoted. In this figure the dimensionless inlet distance $\tilde{m}$, which is equal to the dimensionless distance from the center of the Hertzian contact zone to the inlet edge of the computing area, is shown.

Lubricant starvation can be studied by simply changing the dimensionless inlet distance $\tilde{m}$. A fully flooded condition is said to exist when the dimensionless inlet distance ceases to influence the minimum film thickness to any significant extent.

The value at which the minimum film thickness first starts to change when $\tilde{m}$ is gradually reduced from a fully flooded condition is called the fully flooded - starved boundary position and is denoted by m^*. Therefore lubricant starvation was studied by using the basic elastohydrodynamic lubrication elliptical-contact theory developed in lecture 2 and by observing how reducing the dimensionless inlet distance affected the basic features of the conjunction.

Hard EHL Results

Table 1 shows how changing the dimensionless inlet distance affected the dimensionless minimum film thickness for three groups of dimensionless load and speed parameters. All the data presented in this section are for hard EHL contacts that have a materials parameter G fixed at 4522 and the ellipticity parameter, at 6. It can be seen from table 1 that, as the dimensionless inlet distance $\tilde{m}$ decreases, the dimensionless minimum film thickness H_{min} also decreases.

Table 2 shows how the three groups of dimensionless speed and load parameters considered affected the location of the dimensionless inlet boundary distance m^*. Also given in this table are the corresponding values of dimensionless central and minimum film thickness for the fully flooded condition as obtained by interpolating the numerical values. The value of the dimensionless inlet boundary position m^* shown in table 2 was obtained by using the data from table 1 when the following equation was satisfied:

$$\frac{H_{min} - (H_{min})_{\tilde{m}=m^*}}{H_{min}} = 0.03 \qquad (1)$$

The value of 0.03 was used in equation (1) since it was ascertained that the data in table 1 were accurate to only ±3 percent.

The general form of the equation that describes how the dimensionless inlet distance at the fully flooded - starved boundary m^* varies with the geometry and central film thickness of an elliptical elastohydrodynamic conjunction is given as

$$m^* - 1 = A^* \left[\left(\frac{R_x}{b} \right)^2 H_c \right]^{B^*} \qquad (2)$$

The right side of equation (2) is similar in form to the equations given by Wolveridge, et al. (1971) and Wedeven, et al. (1971). By applying a least-squares power fit to the data obtained from table 1 we can write

$$m^* = 1 + 3.06\left[\left(\frac{R_x}{b}\right)^2 H_c\right]^{0.58} \tag{3}$$

A fully flooded condition exists when $\tilde{m} \geq m^*$, and a starved condition exists when $\tilde{m} < m^*$. The coefficient of determination ϵ for these results is 0.9902, which is entirely satisfactory.

If in equation (2) the dimensionless minimum film thickness is used instead of the central film thickness, we obtain

$$m^* = 1 + 3.34\left[\left(\frac{R_x}{b}\right)^2 H_{min}\right]^{0.56} \tag{4}$$

The coefficient of determination for these results is 0.9869, which is again very good.

Having clearly established the limiting location of the inlet boundary for the fully flooded conditions (eqs. (3) and (4)) we can develop an equation defining the dimensionless film thickness for elliptical conjunctions operating under starved lubrication conditions. The ratio between the dimensionless central film thickness in starved and fully flooded conditions can be expressed in general form as

$$\frac{H_{c,s}}{H_c} = C^*\left(\frac{\tilde{m} - 1}{m^* - 1}\right)^{D^*} \tag{5}$$

Table 3 shows how the ratio of the dimensionless inlet distance parameter to the fully flooded - starved boundary $(\tilde{m} - 1)/(m^* - 1)$ affects the ratio of central film thickness in the starved and fully flooded conditions $H_{c,s}/H_c$. A least-squares power curve fit to the 16 pairs of data points

$$\left[\left(\frac{H_{c,s}}{H_c}\right)_i, \left(\frac{\tilde{m} - 1}{m^* - 1}\right)_i\right], \qquad i = 1, 2, \ldots, 16$$

was used in obtaining values for C^* and D^* in equation (5). For these values of C^* and D^* the dimensionless central film thickness for a starved condition can be written as

$$H_{c,s} = H_c\left(\frac{\tilde{m} - 1}{m^* - 1}\right)^{0.29} \tag{6}$$

By using a similar approach and the data in table 3 the dimensionless minimum film thickness for a starved condition can be written as

$$H_{min,s} = H_{min}\left(\frac{\tilde{m} - 1}{m^* - 1}\right)^{0.25} \tag{7}$$

Therefore, whenever $\tilde{m} < m^*$, where m^* is defined by either equation (3) or (4), a starved lubrication condition exists. When this is true, the dimensionless central film thickness is expressed by equation (6) and the dimensionless minimum film thickness is expressed by equation (7). If $\tilde{m} \geq m^*$, where m^* is defined by either equation (3) or (4), a fully flooded condition exists. Expressions for the dimensionless central and minimum film thicknesses for a fully flooded condition (H_c and H_{min}) were developed in lecture 2.

Figures 2 to 5 explain more fully what happens in going from a fully flooded to a starved lubrication condition. As in lecture 2 the + symbol indicates the center of the Hertzian contact, and the asterisks indicate the Hertzian contact circle. Also on each figure the contour labels and each corresponding value are given.

In figures 2(a), (b), and (c) contour plots of dimensionless pressure ($P = p/E'$) are given for group 1 of table 2 and for dimensionless inlet distances $\tilde{m}$ of 4, 2, and 1.25, respectively. In these figures the contour values are the same in each plot. The pressure spikes are evident in figures 2(a) and (b), but no pressure spike occurs in figure 2(c). This implies that as the dimensionless inlet distance $\tilde{m}$ decreases, or as the severity of lubricant starvation increases, the pressure spike is suppressed. Figure 2(a), with $\tilde{m} = 4$, corresponds to a fully flooded condition; figure 2(b), with $\tilde{m} = 2$, to a starved condition; and figure 2(c), with $\tilde{m} = 1.25$, to even more severe starvation. Once lubricant starvation occurs, the severity of the situation within the conjunction increases rapidly as $\tilde{m}$ is decreased and dry contact conditions are approached.

Contour plots of the dimensionless film thickness ($H = h/R_x$) for the results shown in group 1 of table 2 and for conditions corresponding to the three pressure distributions shown in figure 2 are reproduced in figure 3. It is clear that the film shape in the central region of the elastohydrodynamic conjunction becomes more parallel as lubricant starvation increases and that the region occupied by the minimum film thickness becomes more concentrated. Note also that the values attached to the film thickness contours for the starved condition (fig. 3(c)) are much smaller than those of the film thickness contours for the fully flooded conditions (fig. 3(a)).

In figures 4(a) and (b) the dimensionless pressure ($P = p/E'$) on the X axis is shown for three values of $\tilde{m}$ and for groups 1 and 3 of table 2, respectively. The value of Y was held constant and close to the axis of symmetry of the conjunction for these calculations. The pressure spike diminishes as the severity of starvation increases and dry contact conditions are approached.

In figures 5(a) and (b) the dimensionless film thickness ($H = h/R_x$) on the X axis is shown for three values of $\tilde{m}$ and for groups 1 and 3 of table 2, respectively. Once again the value of Y was held fixed and close to the axis of symmetry of the contact in these calculations. It is clear that the central region becomes flatter as starvation occurs. Also in going from a fully flooded condition to a starved condition the film thickness decreases substantially.

The application of optical interferometry allows the film thickness through the conjunction to be determined experimentally. An example of the interference pattern for a starved, elastohydrodynamically lubricated conjunction is shown in figure 6, which was kindly supplied by Sanborn from the work he reported in 1969. This technique produces information of great clarity and beauty. The film shape of the lubricated conjunction revealed by the experimental results shown in figure 6 compare quite well in qualitative terms with the theoretical results shown in figure 3(c).

Soft EHL Results

By using the theory and numerical procedure mentioned in lecture 2, we can investigate the influence of lubricant starvation on minimum film thickness in starved, elliptical, elastohydrodynamic conjunctions for low-elastic-modulus materials (soft EHL). Lubricant starvation is studied by simply moving the inlet boundary closer to the center of the conjunction, as described in the previous section.

Table 4 shows how the dimensionless inlet distance affects the dimensionless film thickness for three groups of dimensionless load and speed parameters. For all the results presented in this section the dimensionless materials parameter G was fixed at 0.4276, and the ellipticity parameter k was fixed at 6. The results shown in table 4 clearly indicate the adverse effect of lubricant starvation in the sense that, as the dimensionless inlet distance $\tilde{m}$ decreases, the dimensionless minimum film thickness H_{min} also decreases.

Table 5 shows how the three groups of dimensionless speed and load parameters affect the limiting location of the dimensionless critical inlet boundary distance m^*. Also given in this table are corresponding values of the dimensionless minimum film thickness for the fully flooded condition, as obtained by interpolating the numerical values. By making use of table 4 and following the procedure outlined in the previous section, we can write the critical dimensionless inlet boundary distance at which starvation becomes important for low-elastic-modulus materials as

$$m^* = 1 + 1.07\left[\left(\frac{R_x}{b}\right)^2 \tilde{H}_{min}\right]^{0.16} \tag{8}$$

where $\tilde{H}_{min}$ is obtained from the fully flooded soft EHL results given in lecture 2.

Table 6 shows how m^* affects the ratio of minimum film thickness in the starved and fully flooded conditions $\tilde{H}_{min,s}/H_{min}$. The dimensionless minimum film thickness for a starved condition for low-elastic-modulus materials can thus be written as

$$\tilde{H}_{min,s} = H_{min}\left(\frac{\tilde{m} - 1}{m^* - 1}\right)^{0.22} \tag{9}$$

Therefore, whenever $\tilde{m} < m^*$, where m^* is defined by equation (8), a lubricant starvation condition exists. When this is true, the dimensionless minimum film thickness is expressed by equation (9). If $\tilde{m} \geq m^*$, a fully flooded condition exists, and the expression for the dimensionless minimum film thickness for a fully flooded condition H_{min} for materials of low elastic modulus was developed in lecture 2.

In figure 7 contour plots of the dimensionless pressure ($P = p/E'$) are shown for the group 3 conditions recorded in table 4 and for dimensionless inlet distances of 1.967, 1.333, and 1.033. Note that the contour levels and intervals are identical in all parts of figure 7. In figure 7(a), with $\tilde{m} = 1.967$, an essentially fully flooded condition exists. The contours are almost circular and extend farther into the inlet region than into the exit region. In figure 7(b), with $\tilde{m} = 1.333$, starvation is influencing the distribution of pressure, and the inlet contours are slightly less circular than those shown in figure 7(a). By the time $\tilde{m}$ falls to 1.033 (fig.

7(c)), the conjunction is quite severely starved and the inlet contours are even less circular.

In figure 8 contour plots of the dimensionless film thickness ($H = h/R_x$) are shown, also for the group 3 conditions recorded in table 4 and for dimensionless inlet distances of 1.967, 1.333, and 1.033. These film thickness results correspond to the pressure results shown in figure 7. The central portion of the film thickness contours becomes more parallel as starvation increases and the minimum-film-thickness area moves to the exit region. The values of the film thickness contours for the most starved condition (fig. 8(c)) are much lower than those for the fully flooded condition (fig. 8(a)).

CONCLUDING REMARKS

The influence of lubricant starvation on minimum film thickness in starved, elliptical, elastohydrodynamically lubricated conjunctions was investigated for materials of high and low elastic modulus (hard and soft EHL, respectively). Lubricant starvation was studied by moving the inlet boundary closer to the center of the conjunction in the numerical solutions. The results show that the location of the dimensionless critical inlet boundary distance m^* between the fully flooded and starved conditions can be expressed simply as

<u>For hard EHL</u>

$$m^* = 1 + 3.34\left[\left(\frac{R_x}{b}\right)^2 H_{min}\right]^{0.56}$$

<u>For soft EHL</u>

$$m^* = 1 + 1.07\left[\left(\frac{R_x}{b}\right)^2 H_{min}\right]^{0.16}$$

That is, for a dimensionless inlet distance $\tilde{m}$ less than m^*, starvation occurs and, for $\tilde{m} \geq m^*$, a fully flooded condition exists. Furthermore it has been possible to express the minimum film thickness for a starved condition as

<u>For hard EHL</u>

$$H_{min,s} = H_{min}\left(\frac{\tilde{m} - 1}{m^* - 1}\right)^{0.25}$$

<u>For soft EHL</u>

$$H_{min,s} = H_{min}\left(\frac{\tilde{m} - 1}{m^* - 1}\right)^{0.22}$$

Contour plots of pressure and film thickness in and around both hard and soft EHL contacts have been presented for both fully flooded and starved lubrication conditions. It is evident from the hard EHL contact results that as the severity of starvation increases, the pressure spike becomes suppressed, the film shape becomes more nearly parallel over a substantial part of the Hertzian contact ellipse, and the film thickness decreases substantially. From the soft EHL results it is evident that the inlet pressure contours becomes less circular and closer to the edge of the Hertzian contact zone and that the film thickness decreases substantially as the severity of starvation increases.

APPENDIX - SYMBOLS

b	semiminor axis of contact ellipse, m
E	modulus of elasicity, N/m^2
E'	effective elastic modulus, $2\Big/\left[\dfrac{1-\nu_a^2}{E_a}+\dfrac{1-\nu_b^2}{E_b}\right]$, N/m^2
F	normal applied load, N
G	dimensionless materials parameter, $\alpha E'$
H	dimensionless film thickness, h/R_x
$\tilde{H}$	dimensionless film thickness obtained from least-squares fit of numerical data
h	film thickness, m
k	ellipticity parameter
$\tilde{m}$	dimensionless inlet distance (fig. 1)
m^*	dimensionless inlet distance at boundary between fully flooded and starved conditions
P	dimensionless pressure, p/E'
p	pressure, N/m^2
R	effective radius, m
r	radius of curvature, m
U	dimensionless speed parameter, $\eta_0 u/E'R_x$
u	mean surface velocity in direction of motion, $(u_a + u_b)/2$, m/s
W	dimensionless load parameter, $F/E'R_x^2$
x,y,X,Y	coordinate system
α	pressure-viscosity coefficient of lubricant, m^2/N
η_0	viscosity at atmospheric pressure, $N\ s/m^2$
ν	Poisson's ratio

Subscripts:

a	solid a
b	solid b
c	central
min	minimum
s	starved
x,y	coordinate system

REFERENCES

Castle, P. and Dowson, D. (1972) "A Theoretical Analysis of the Starved Elastohydrodynamic Lubrication Problem for Cylinders in Line Contact." Proceedings of the Second Symposium on Elastohydrodynamic Lubrication, Institution of Mechanical Engineers (London), 131.

Grubin, A. N. (1949) "Fundamentals of the Hydrodynamic Theory of Lubrication of Heavily Loaded Cylindrical Surfaces," Investigation of the Contact Machine Components. Kh. F. Ketova, ed., Translation of Russian Book No. 30, Central Scientific Institute for Technology and Mechanical Engineering, Moscow, Chapter 2. (Available from Dept. of Scientific and Industrial Research, Great Britian, Transl. CTS-235, and from Special Libraries Association, Chicago, Transl. R-3554.)

Hamrock, B. J. and Dowson, D. (1977) "Isothermal Elastohydrodynamic Lubrication of Point Contacts. Part IV - Starvation Results," J. Lubr. Technol., 99 (1), 15-23.

Hamrock, B. J. and Dowson, D. (1979) "Elastohydrodynamic Lubrication of Elliptical Contacts for Materials of Low Elastic Modulus. Part II - Starved Conjunction." J. Lubr. Technol., 101 (1), 92-98.

Orcutt, F. K. and Cheng, H. S. (1966) "Lubrication of Rolling-Contact Instrument Bearings," Gyro-Spin Axis Hydrodynamic Bearing Symposium, Vol. 2, Ball Bearings, Massachusetts Institute of Technology, Cambridge, Mass., Tab. 5.

Sanborn, D. M. (1969) "An Experimental Investigation of the Elastohydrodynamic Lubrication of Point Contacts in Pure Sliding," Ph. D. Thesis, University of Michigan.

Wedeven, L. E., Evans, D., and Cameron, A. (1971) "Optical Analysis of Ball-Bearing Starvation," J. Lubr. Technol., 93 (3), 349.

Wolveridge, P. E., Baglin, K. P., and Archard, J. G. (1971) "The Starved Lubrication of Cylinders in Line Contact," Proc. Inst. Mech. Eng. (London), 185 (1), 1159-1169.

TABLE 1. - EFFECT OF STARVATION ON MINIMUM FILM THICKNESS FOR HARD EHL CONTACTS

Dimensionless Inlet Distance, $\tilde{m}$	Group 1	Group 2	Group 3
	Dimensionless Load Parameter, W		
	0.3686×10^{-6}	0.7371×10^{-6}	0.7371×10^{-6}
	Dimensionless Speed Parameter, U		
	0.1683×10^{-11}	1.683×10^{-11}	5.050×10^{-11}
	Minimum Film Thickness, H_{min}		
6	----------	29.75×10^{-6}	61.32×10^{-6}
4	6.317×10^{-6}	29.27	57.60
3	6.261	27.84	51.70
2.5	----------	26.38	46.89
2	5.097	23.40	39.01
1.75	----------	21.02	34.61
1.5	4.236	----------	27.00
1.25	3.945	----------	----------

TABLE 2. - EFFECT OF DIMENSIONLESS SPEED AND LOAD PARAMETERS ON DIMENSIONLESS INLET DISTANCE AT FULLY FLOODED - STARVED BOUNDARY FOR HARD EHL CONTACTS

Group	Dimensionless Parameters			Fully Flooded Film Thickness		Dimensionless Inlet Boundary, m^*
	U	W	R_x/b	Central, H_c	Minimum, H_{min}	
1	0.1683×10^{-11}	0.3686×10^{-6}	205.9	7.480×10^{-6}	6.211×10^{-6}	2.62
2	1.683	.7371	163.5	33.55	29.20	3.71
3	5.050	.7371	163.5	70.67	60.02	5.57

TABLE 3. - EFFECT OF DIMENSIONLESS INLET DISTANCE ON DIMENSIONLESS CENTRAL- AND MINIMUM-FILM-THICKNESS RATIOS FOR HARD EHL CONTACTS

Group	Dimensionless Inlet Distance, $\tilde{m}$	Film Thickness Ratios for Starved and Flooded Conditions: Central, $H_{c,s}/H_c$	Film Thickness Ratios for Starved and Flooded Conditions: Minimum, $H_{min,s}/H_{min}$	Inlet Boundary Parameters: Critical, $\frac{\tilde{m}-1}{m^*-1}$	Inlet Boundary Parameters: Wedeven, et al. (1971), $\frac{\tilde{m}-1}{m_W-1}$
1	2.62	1	1	1	0.9893
	2	.9430	.9640	.6173	.6108
	1.5	.7697	.8417	.3086	.3054
	1.25	.5689	.6311	.1543	.1527
2	3.71	1	1	1	0.8281
	3	.9574	.9534	.7380	.6111
	2.5	.8870	.9034	.5525	.4584
	2	.7705	.8034	.3693	.3056
	1.75	.7151	.7199	.2768	.2292
3	5.57	1	1	1	0.8498
	4	.9348	.9439	.6565	.5570
	3	.8330	.8487	.4370	.3719
	2.5	.7440	.7607	.3282	.2789
	2	.6223	.6551	.2188	.1860
	1.75	.5309	.5681	.1641	.1395
	1.5	.4165	.4580	.1094	.0930

TABLE 4. - EFFECT OF STARVATION ON FILM THICKNESS FOR SOFT EHL CONTACTS

Dimensionless Inlet Distance, $\tilde{m}$	Group 1	Group 2	Group 3
	Dimensionless Load Parameter, W		
	0.4405×10^{-3}	0.2202×10^{-3}	0.4405×10^{-3}
	Dimensionless Speed Parameter, U		
	0.5139×10^{-8}	0.1027×10^{-7}	0.5139×10^{-7}
	Dimensionless Minimum Film Thickness, H_{min}		
1.967	131.8×10^{-6}	241.8×10^{-6}	584.7×10^{-6}
1.833	131.2	238.6	572.0
1.667	129.7	230.8	543.1
1.500	125.6	217.2	503.0
1.333	115.9	199.3	444.9
1.167	98.11	120.8	272.3
1.033	71.80	120.8	272.3

TABLE 5. - EFFECT OF INLET DISTANCE ON FILM THICKNESS

FOR SOFT EHL CONTACTS

Group	Dimensionless Parameters			Fully Flooded Minimum Film Thickness, H_{min}	Dimensionless Inlet Boundary, m^*
	U	W	R_x/b		
1	0.6130×10^{-8}	0.4405×10^{-3}	10.41	127.8×10^{-6}	1.661
2	$.1027\times10^{-7}$	.2202	24.45	234.5	1.757
3	.2130	.4405	10.41	567.2	1.850

TABLE 6. - EFFECT OF INLET DISTANCE ON MINIMUM-

FILM-THICKNESS RATIO FOR SOFT EHL CONTACTS

Group	Dimensionless Inlet Distance, $\tilde{m}$	Ratio of Minimum Film Thicknesses for Starved and Flooded Conditions, $H_{min,s}/H_{min}$	Critical Inlet Boundary Parameter, $(\tilde{m} - 1)/(m^* - 1)$
1	1.661	1	1
	1.500	.9928	.7564
	1.333	.9069	.5038
	1.167	.7677	.2526
	1.033	.5618	.0499
2	1.757	1	1
	1.667	.9842	.8811
	1.500	.9202	.6605
	1.333	.8409	.4399
	1.167	.7207	.2206
	1.033	.5151	.0436
3	1.850	1	1
	1.667	.9575	.7847
	1.500	.8868	.5882
	1.333	.7844	.3918
	1.167	.6761	.1963
	1.033	.4801	.0388

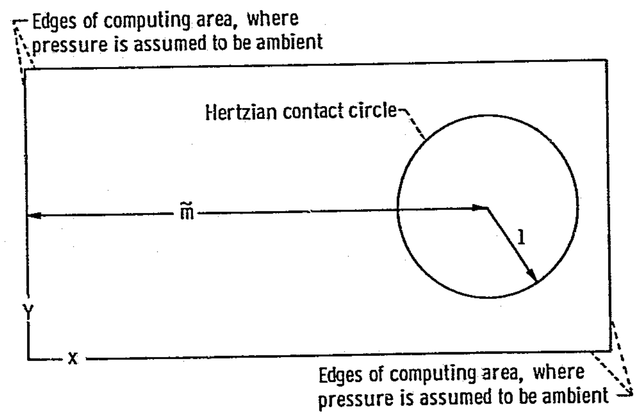

Figure 1. - Computing area in and around Hertzian contact zone.

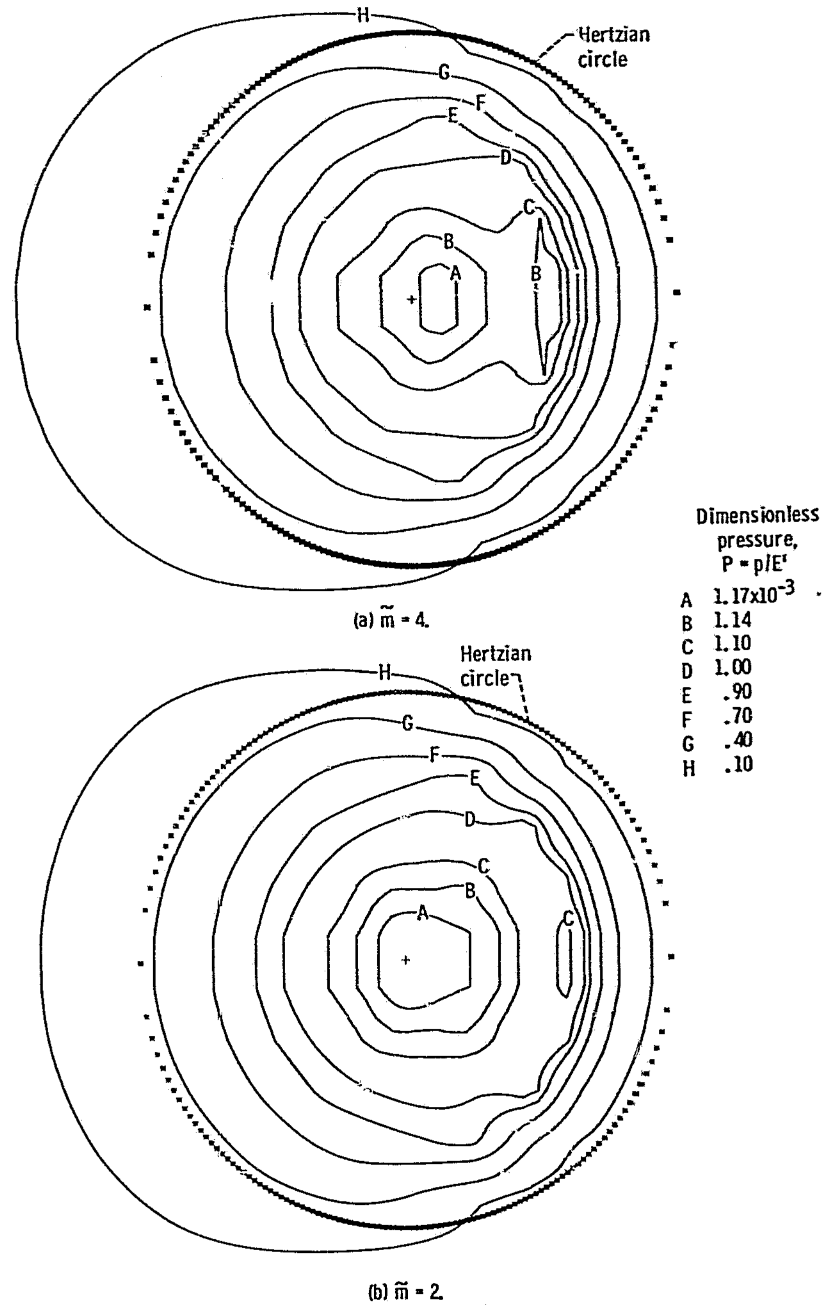

Figure 2. - Contour plots of dimensionless pressure for dimensionless inlet distances $\tilde{m}$ of 4, 2, and 1.25 and for group 1 of table 2.

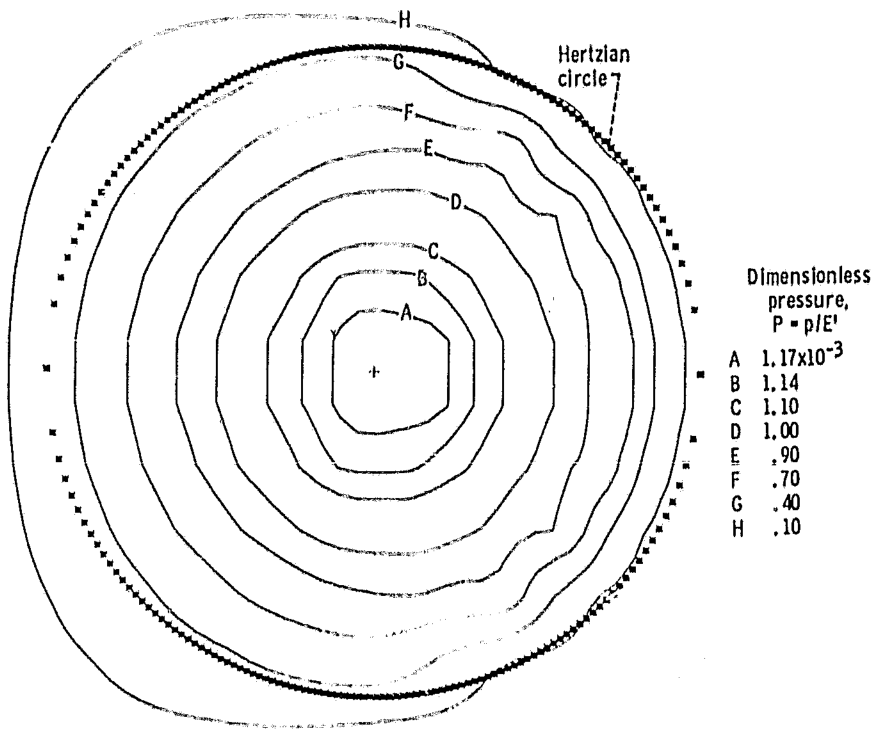

(c) $\tilde{m}$ = 1.25.

Figure 2. - Concluded.

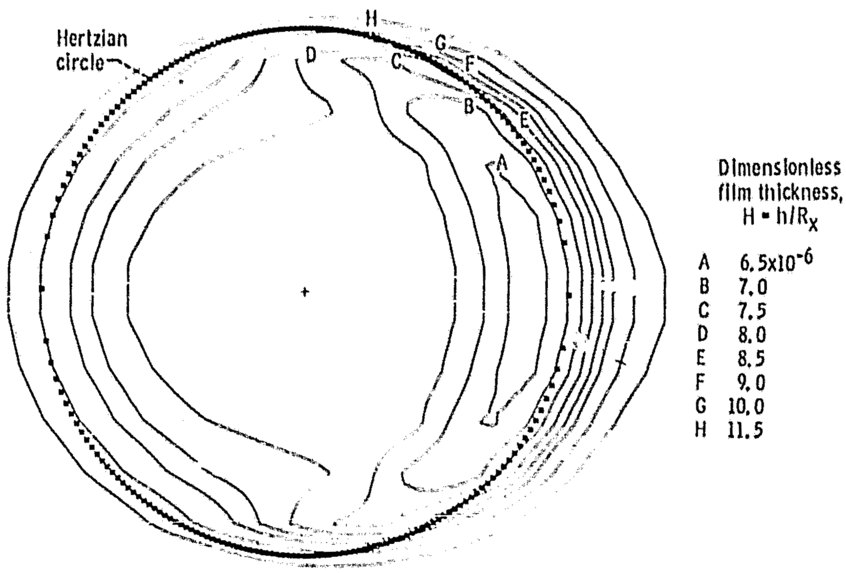

(a) $\tilde{m} = 4$.

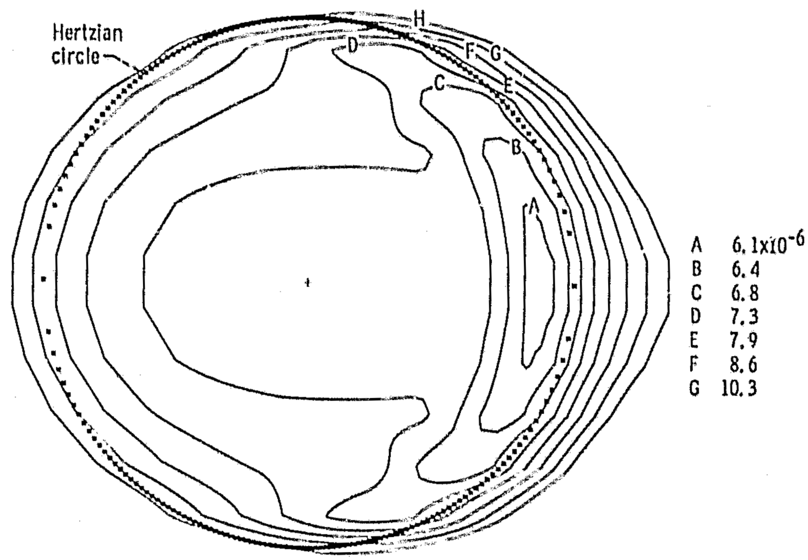

(b) $\tilde{m} = 2$.

Figure 3. - Contour plots of dimensionless film thickness for dimensionless inlet distances $\tilde{m}$ of 4, 2, and 1.25 and for group 1 of table 2.

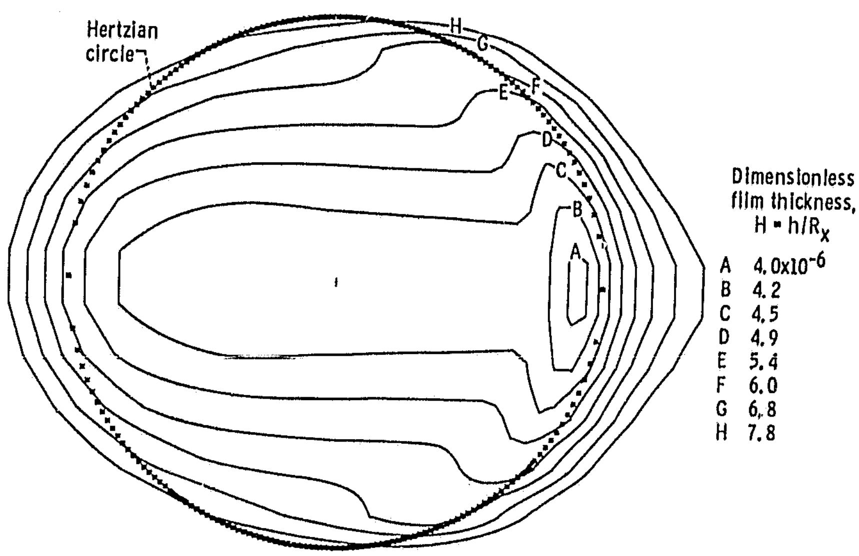

(c) $\tilde{m} = 1.25$.

Figure 3. - Concluded.

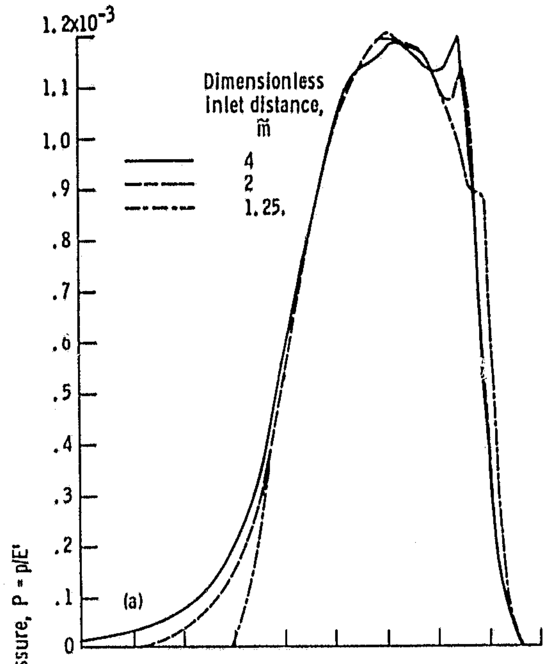

(a) Dimensionless parameters U and W held constant as given in group 1 of table 2.

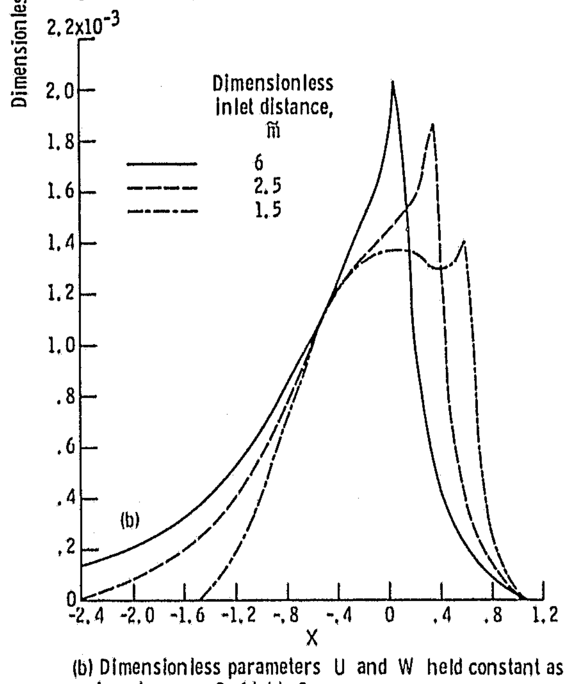

(b) Dimensionless parameters U and W held constant as given in group 3 of table 2.

Figure 4. - Dimensionless pressure on X-axis for three values of dimensionless inlet distance. The value of Y is held fixed near axial center of contact.

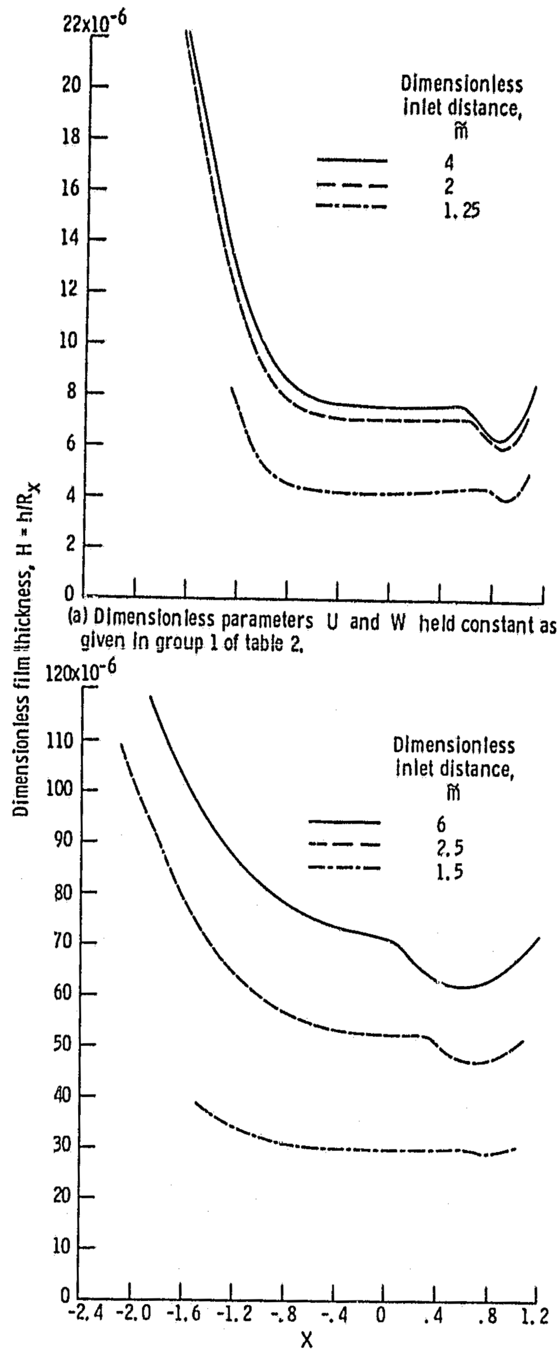

(a) Dimensionless parameters U and W held constant as given in group 1 of table 2.

(b) Dimensionless parameters U and W held constant as given in group 3 of table 2.

Figure 5. - Dimensionless film thickness on X-axis for three values of dimensionless inlet distance. The value of Y is held fixed near axial center of contact.

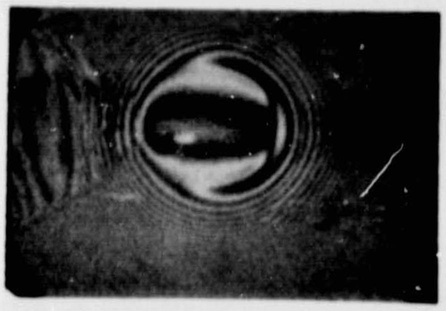

Figure 6. - Interference pattern for a starved elastohydrodynamic lubricated conjunction. (From Sanborn, 1969.)

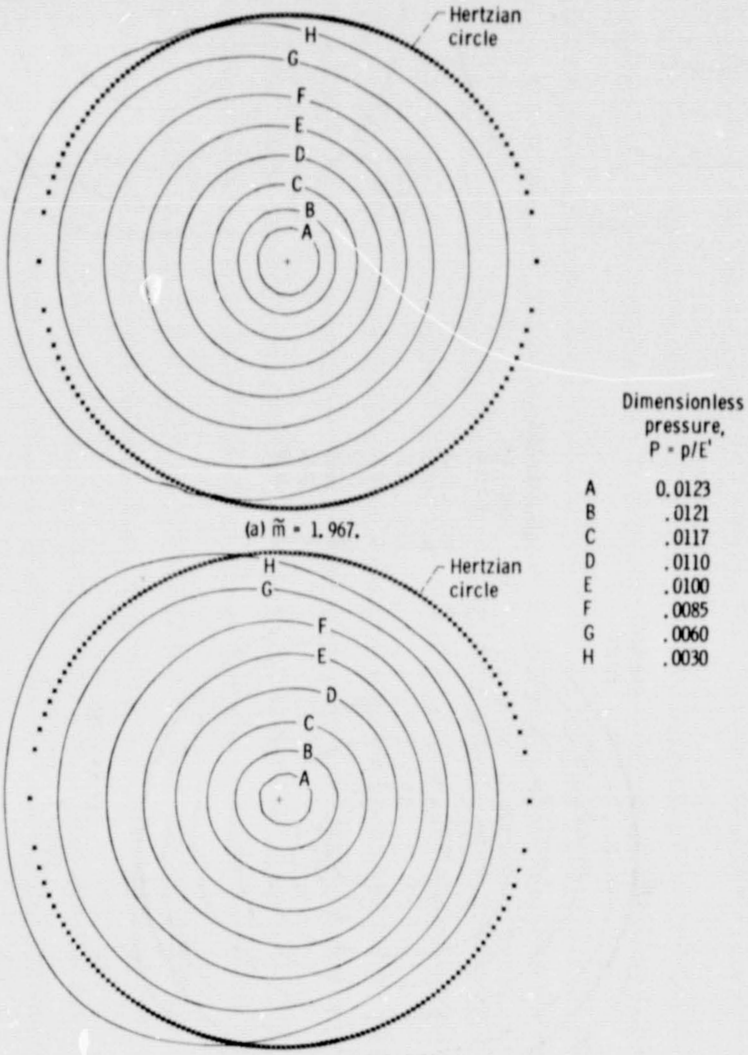

(a) $\tilde{m}$ = 1.967.

(b) $\tilde{m}$ = 1.333.

Figure 7. - Contour plots of dimensionless pressure for dimensionless inlet distances $\tilde{m}$ of 1.967, 1.333, and 1.033 and for group 3 of table 4.

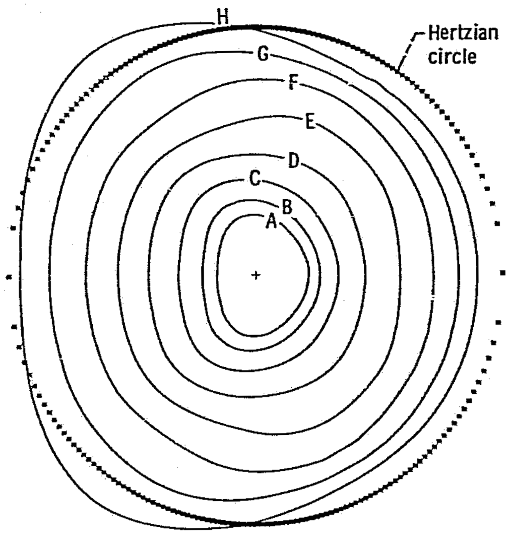

(c) $\tilde{m}$ = 1.033.

Figure 7. - Concluded.

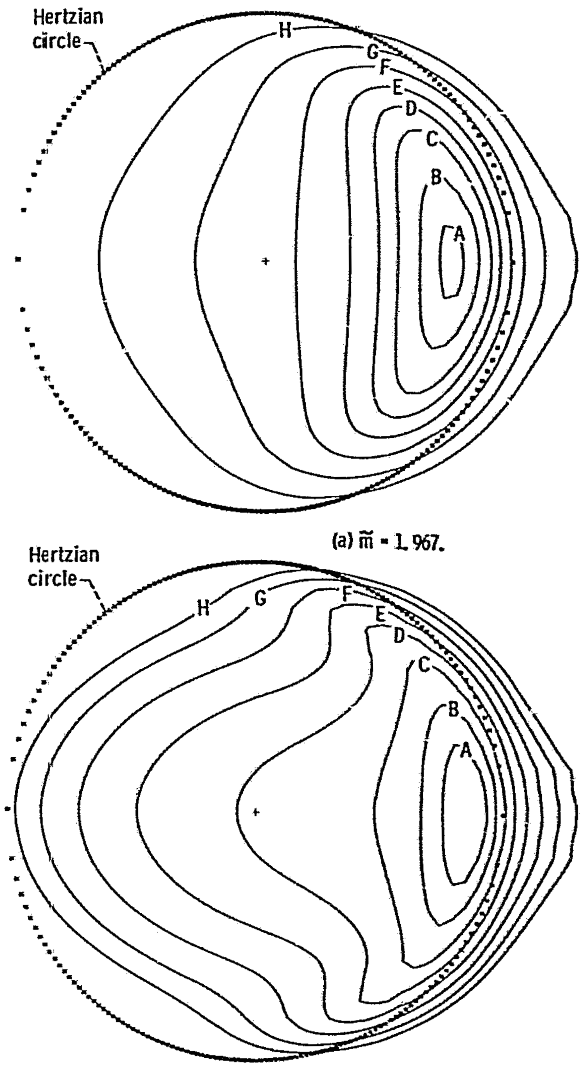

(b) $\tilde{m}$ = 1.333.

Figure 8. - Contour plots of dimensionless film thickness for dimensionless inlet distances $\tilde{m}$ of 1.967, 1.333, and 1.033 and for group 3 of table 4.

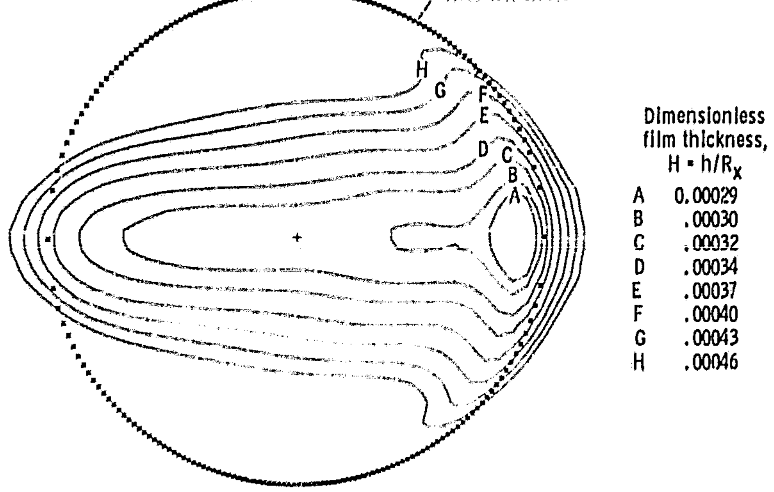

(c) $\tilde{m} = 1.033$.

Figure 8. - Concluded.